Review

The Aharonov-Bohm effect and its applications to electron phase microscopy

By Akira TONOMURA*), **), ***), ****), †)

(Communicated by Jun KONDO, M. J. A.)

Abstract: The Aharonov-Bohm effect was conclusively established by a series of our electron interference experiments, with the help of some advanced techniques, such as coherent field-emission electron beams and microlithography. Using this fundamental principle behind the interaction of an electron wave with electromagnetic fields, new observation techniques were developed to directly observe microscopic objects and quantum phenomena previously unobservable.

Key words: The Aharonov-Bohm effect; electron microscopy; electron wave interference; magnetic lines of force; vortex; superconductor.

Introduction. Electron beams are influenced by electromagnetic fields in the form of the beam deflection caused by Lorentz forces, but can also show wave properties in microscopic regions: The way the electron wave behaves can be described with the Schrödinger equation. This equation tells us that, even when an electron beam passing through electromagnetic fields is only slightly influenced in its path, the electron beam is influenced as a change not in its intensity but in its phase. In the regions where electron beams behave as waves, the concept of the forces is no longer relevant, and therefore, that of electric fields $\boldsymbol{E}$ and magnetic fields $\boldsymbol{B}$ defined as forces acting on a unit charge, takes on a secondary meaning. Instead of forces, "phase shifts" come into play. The primary physical entities are neither $\boldsymbol{E}$ nor $\boldsymbol{B}$, but electrostatic potentials V and vector potentials $\boldsymbol{A}$, since these potentials directly produce the phase shifts.

In 1959, Y. Aharonov and D. Bohm[1),2)] theoretically predicted that a relative phase shift can exist even when the electron beams pass only through spaces free of $\boldsymbol{E}$ and $\boldsymbol{B}$. This effect was later called "the Aharonov-Bohm effect". They attributed this effect to potentials, V and $\boldsymbol{A}$, which are considered to have no physical meaning in classical physics.

The AB effect increased in significance in the 1970s in relation to the unified theories of all fundamental interactions in nature, where potentials are extended to "gauge fields" and regarded as the most fundamental physical quantity. In fact, T. T. Wu and C. N. Yang[3)] stressed the significance of the AB effect in relation to the physical reality of gauge fields (potentials) as follows:

> The concept of an SU_2 gauge field was first discussed in 1954. In recent years many theorists, perhaps a majority, believe that SU_2 gauge fields do exist. However, so far there is no experimental proof of this theoretical idea, since conservation of isotopic spin only suggests, and does not require, the existence of an isotopic spin gauge field. What kind of experiment would be a definitive test of the existence of an isotopic spin gauge field? A generalized Bohm-Aharonov experiment would be.

However, since potentials have long been regarded as mathematical auxiliaries, some people questioned the existence of the AB effect, thus causing a controversy.[4),5)] Although the AB effect had been experimentally tested[6)-9)] to exist for the magnetic case soon after its

*) Advanced Research Laboratory, Hitachi, Ltd., Saitama, Japan.
**) Frontier Research System, RIKEN, Saitama, Japan.
***) Okinawa Institute of Science and Technology, Promotion Corporation Initial Research Project, Okinawa, Japan.
****) Recipient of the Imperial Prize and the Japan Academy Prize in 1991.
†) Advanced Research Laboratory, Hitachi, Ltd., 2520, Akanuma, Hatoyama, Saitama 350-0395, Japan (tonomura@harl.hitachi.co.jp).

Table I. History of development of bright electron beams

Years	Electron microscopes	Brightness ($A/cm^2 \cdot ster$)	Application
1968	100-KVEM (Thermionic electrons)	1×10^6	Experimental feasibility of electron holography[24]
1978	80-KV FEEM	1×10^8	Direct observation of magnetic lines of force[16]
1982	250-KV FEEM	4×10^8	Conclusive experiments of AB effect[14]
1989	350-KV FEEM	5×10^9	Dynamic observation of vortices in metal superconductors[22]
2000	1-MV FEEM	2×10^{10}	Observation of unusual behaviors of vortices in high-T_c superconductors[23),28]

* FEEM: field-emission electron microscope

prediction, these results were attributed to the effect of magnetic fields leaking from both ends of finite solenoids or ferromagnets used in the experiments.[10),11]

We made a series of experiments[12)-15] using tiny leakage-free magnetic samples of toroidal geometry and in addition, by quantitatively measuring precision in leakage-free conditions using holographic interference microscopy.[16),17] By the last experiment[14] using a toroidal magnet covered with superconductors, which C. G. Kuper[18] and C. N. Yang[19] proposed, the existence of the AB effect was conclusively confirmed.

We also used the underlying principle of the AB effect to quantitatively observe magnetic lines of force[16),20] and quantized vortices in superconductors[21] as electron interference micrographs, and also to dynamically observe the movements of vortices[22),23] by Lorentz microscopy (out-of-focus transmission electron microscopy). In this paper, we review these experimental results on the AB effect and its applications using coherent electron beams we developed over the past 40 years.

Historical developments of coherent electron beams. We started our research on electron holography in 1968[24] as a way to overcome the saturated state of electron microscopy technology. However, we were convinced from the experiments that bright electron beams, such as laser beams in optics, would be needed to practically apply interference techniques, including electron holography.

We soon began developing bright and yet monochromatic electron beams that are field-emitted from a pointed tip, and we have continued to do so. Since this electron source is extremely small, typically 50 Å in diameter, it has to be immobile even by a fraction of the source diameter. Therefore, we had to overcome these technical difficulties to prevent even the slightest mechanical vibration of the tip, the accelerating tube, and the microscope column, or the slightest deflection of the fine beam by stray ac magnetic fields. Otherwise, the inherent high brightness of the electron beam would deteriorate.

After ten years of work, we developed an 80-kV electron beam,[25] which was two orders of magnitude brighter than that of the then used thermal beams (see Table I). Electron interference patterns became directly observable on the fluorescent screen and as many as 3000 interference fringes were recorded on film. By using electron holography and bright electron beams, new information that could not be obtained by conventional electron microscopy was obtainable. For example, magnetic lines of force inside and outside ferromagnetic samples were directly and quantitatively observed in h/e flux units[16),20] in interference micrographs, which can be obtained in the optical reconstruction stage of off-axis electron holography.

Even after that, we continued to develop even brighter electron beams. As shown in Table I, a series of experiments on the AB effect[12)-15] were carried out with a 250-kV electron microscope, magnetic vortices in metal superconductors[22] were observed with a 350-kV microscope,[26] and unusual behaviors of vortices peculiar to high-T_c superconductors[23),27),28] were observed with a 1-MV microscope.[29] These observations became possible by precisely detecting the phase of an electron wave using bright electron beams.

Phase of an electron wave. Phase shifts of an electron wave transmitted through the electromagnetic fields, V and $\boldsymbol{A}$, can be derived from the Schrödinger equation. The phase S of an electron wave, especially when electromagnetic fields are weak enough for the

WKB approximation to be valid, can simply be expressed as follows:

$$S = \frac{1}{\hbar}\int(\mathrm{m}\boldsymbol{v} - \mathrm{e}\boldsymbol{A})\,\mathrm{d}\boldsymbol{s}, \qquad [1]$$

where the line integral is carried out along an electron path. The effect of electrostatic potentials V is included in $\boldsymbol{v}$. Conversely, this eq. [1] can also give us the definition of electromagnetic potentials.

It can be physically understood from Eq. [1] how electromagnetic potentials influence the electron phase. The first term, $\int \mathrm{m}\boldsymbol{v}\ \mathrm{d}\boldsymbol{s}/\hbar$ in this equation corresponds to the optical path length. The effect of vector potentials $\boldsymbol{A}$ cannot be included in this term, but is given by the second term.

By comparing these two terms, $-\mathrm{e}\boldsymbol{A}$ can be interpreted as a kind of electron momentum. In exact terms, $-\mathrm{e}\boldsymbol{A}$ is the momentum exchanged between the sources of the fields and an electron, and exists only because an electron has an electric charge, irrespective of whether it is at rest or moving. In fact, if a unit charge is placed in a magnetic field, the integral value of the field momentum (the vector product between electric and magnetic fields, $\boldsymbol{E} \times \boldsymbol{B}$) over all the space becomes equal to the vector potential $\boldsymbol{A}$ at the point of the charge.[30]

The Aharonov-Bohm effect. The effect of potentials was theoretically predicted observable by the AB effect.[1),2)] There are two kinds of AB effect, electric and magnetic.[1)] In the magnetic AB effect, an electron beam having passed through the field-free regions on both sides of an infinitely long solenoid is physically influenced as a displacement of interference fringes (Fig. 1). The fringe displacement was attributed to the vector potentials, which are directed in the opposite directions on both sides of the solenoid for the Coulomb gauge, and shift the phases of the electron beams passing through on both sides differently. The vector potentials, and also the phase S, are not uniquely determined for a given physical situation, but have an arbitrariness of gauge transformation. However, it does not mean that vector potentials and electron phases have no physical significance. It is true that the phase S can have arbitrary values. However, what can be observed experimentally is a relative phase shift ΔS between two beams starting from a point source, passing through electromagnetic potentials, and ending at another point. This ΔS, which can be observed from the interference pattern, is given by,

$$\Delta S = \frac{1}{\hbar}\oint(\mathrm{m}\boldsymbol{v} - \mathrm{e}\boldsymbol{A})\,\mathrm{d}\boldsymbol{s}. \qquad [2]$$

This time the integral is carried out along a closed path determined by connecting the two electron paths.

In a pure magnetic case,

$$\Delta S = \frac{e}{\hbar}\oint \boldsymbol{A}\,\mathrm{d}\boldsymbol{s} = -\frac{e}{\hbar}\int \boldsymbol{B}\,\mathrm{d}\boldsymbol{S}, \qquad [3]$$

where the latter surface integral is performed over the surface bordered by the closed path. Since ΔS is thus proportional to the magnetic flux passing through the closed path, it is uniquely determined.

The AB effect became regarded as a fundamental in quantum mechanics and furthermore increased in significance in relation to the unified theories of gauge fields in the 1970s.

However, in 1978, the existence of the AB effect had been questioned[4)] and controversy about it has arisen.[5)]

Controversy on the existence of the AB effect. Discussions on the physical reality of potentials, dates back to the days of M. Faraday and J. C. Maxwell.[31)] Faraday took into consideration the law of electromagnetic induction he himself discovered, that states electric and magnetic fields, $\boldsymbol{E}$ and $\boldsymbol{B}$, were not independent quantities, but that there must exist more fundamental quantities connecting them, which he called the "electrotonic state".

However, Faraday never found out what they were. It was Maxwell who built upon this idea. In 1856, he found that Faraday's electrotonic state could be described by vector potentials as follows in today's notation[32)]:

$$\boldsymbol{B} = \mathrm{rot}\,\boldsymbol{A}, \text{ and} \qquad [4]$$

$$\boldsymbol{E} = -\frac{\mathrm{d}\boldsymbol{A}}{\mathrm{d}t}. \qquad [5]$$

These equations tell us that both magnetic field $\boldsymbol{B}$ and electric field $\boldsymbol{E}$ can be obtained from vector potential $\boldsymbol{A}$. A magnetic field $\boldsymbol{B}$ is produced when the spatial distribution of $\boldsymbol{A}$ has a rotation, or a vortex. An electric field $\boldsymbol{E}$ is produced when $\boldsymbol{A}$ changes with time. Maxwell believed vector potential $\boldsymbol{A}$ to be the most fundamental quantity in electromagnetism, and, in fact, called $\boldsymbol{A}$ "electromagnetic momentum".

However, O. Heaviside[33)] and H. R. Hertz,[34)] when they reformulated Maxwell's equations, threw away the vector potentials $\boldsymbol{A}$. Since that time, $\boldsymbol{A}$ has been regard-

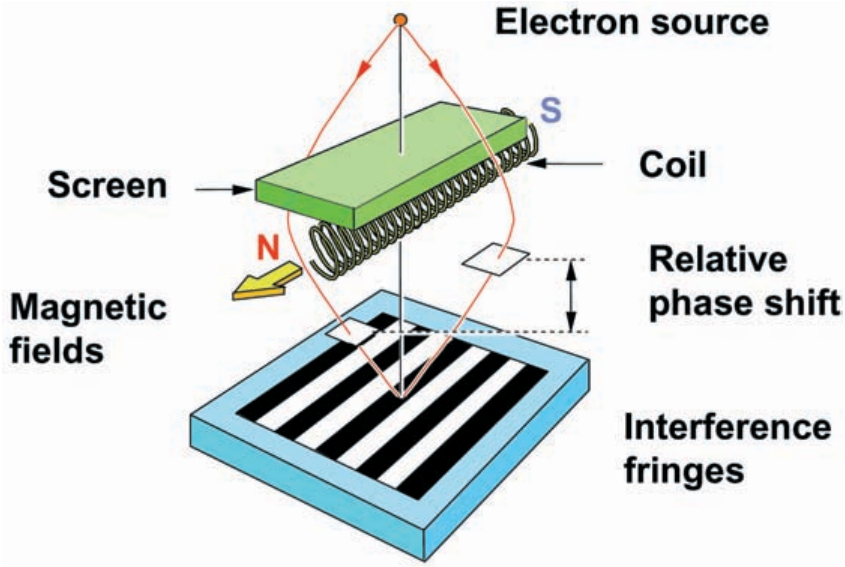

Fig. 1. The Aharonov-Bohm effect.

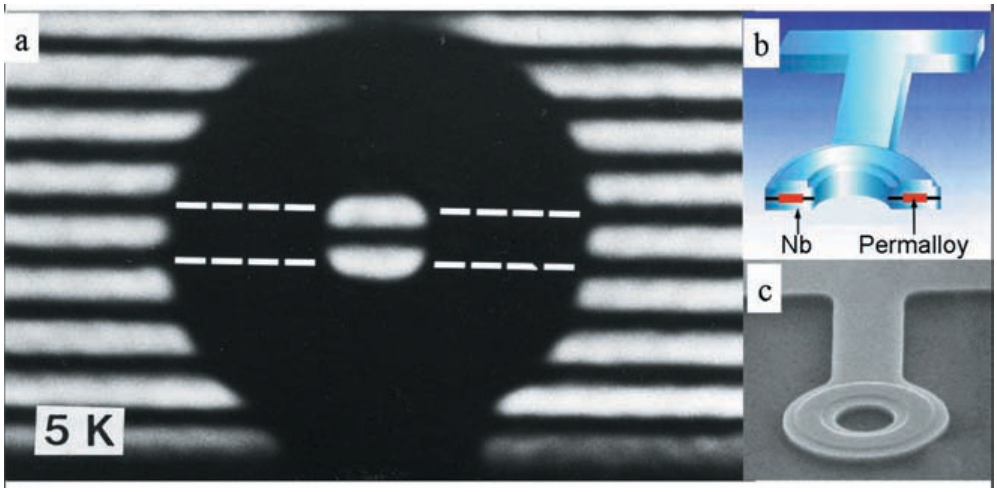

Fig. 2. Conclusive experiment of the Aharonov-Bohm effect. (a) Interference pattern indicating the existence of a non-zero relative phase shift. (b) Schematic of a toroidal sample covered with superconductor. (c) Scanning electron micrograph.

ed as a mathematical quantity that has no physical meaning and is convenient only for calculations.

Vector potentials began to enter the central stage of physics again when a gauge theory was introduced by H. Weyl[35] as a unified theory of gravity and electromagnetism, although his theory was rejected by A. Einstein to produce an unrealistic result. Weyl assumed that his gauge fields, or vector potentials, changed the scale of space-time, but in a new gauge theory established after the advent of quantum mechanics it became evident that vector potentials change the phase S of electrons. The unrealistic result pointed out by Einstein was found to correspond to the AB effect in this new gauge theory.

After this gauge theory became the most probable candidate for a unified theory, there arose a controvery over the existence of the AB effect.

We attempted to gather conclusive evidence for it, since the AB effect was also the fundamental principle behind our method of observing magnetic lines of force. We had to continue to conduct a series of experiments on the AB effect until 1986,[12)-15)] since repeated objections arose about our results during the controversy.

Confirmation experiments on the AB effect. We carried out a series of experiments to clarify any ambiguities raised in the controversy, and we introduce here the last experiment,[14)] which is considered to be the most conclusive. We used a toroidal ferromagnet instead of a straight solenoid, which has inevitable leakage fluxes from both ends of the solenoid. An infinite solenoid is experimentally unattainable, but an ideal geometry with no flux leakage can be achieved by the finite system of a toroidal magnetic field.[18)] Furthermore, the toroidal ferromagnet was covered with a superconducting niobium layer to completely confine the magnetic field.

An electron wave was incident to a tiny toroidal sample fabricated using the most advanced lithography techniques, and the relative phase shift ΔS between two waves passing through the hole and around the toroid was measured as an interferogram.

Although samples that had various magnetic flux values were measured, the ΔS was either 0 or π. The conclusion is now obvious. The photograph in Fig. 2 indicates that a relative phase shift of π is produced, indicating the existence of the AB effect even when the magnetic fields are confined within the superconductor and shielded from the electron wave. An electron wave must be physically influenced by the vector potentials.

In this experiment a quantization of the relative phase shift, either 0 or π, assured that the niobium layer surrounding the magnet actually became superconductive. When a superconductor completely surrounds a magnetic flux, the flux is quantized to an integral multiple of quantized flux, $h/(2e)$. When an odd number of vortices are enclosed inside the superconductor, the relative phase shift becomes π (mod. 2π). For an even number of vortices, the phase shift is 0. Therefore, the occurrence of flux quantization can be used to confirm that the niobium layer actually became superconductive, that the superconductor completely surrounded the magnetic flux, and that the Meissner effect prevented any flux from leaking out. Therefore, we can conclude that electron waves passing through the field-free regions inside and outside the toroidal magnet are phase-shifted by π, although the waves never touch the magnetic fields.

Soon after the AB effect was conclusively confirmed by a series of experiments using electron beams, electrons inside metals were also found to show the AB effect.

R. A. Webb of IBM used a tiny ring circuit to demonstrate that electrons inside metals also show interference and the AB effect.[36)] When 100 electrons enter a ring circuit, it is a matter of course in classical physics that 100 electrons exit. However, they now behave as waves, and even a single electron can split into two partial waves. Therefore, the number of electrons that exit the ring can become 10 or 190 because of constructive or destructive interference, depending on their relative phases. Therefore, when magnetic flux passes through the ring circuit and changes the relative electron phase between the two partial waves due to the AB effect, the electron current, or the resistance, oscillates.

The AB effect was detected also in carbon nanotubes.[37)] In a cylinder, electrons can take many different paths to get from one point to another along the axis of the cylinder; a direct route or a right or left-handed path. If magnetic flux passes through this cylinder, their relative phase changes due to the AB effect, thus change the resistance. Ohm's law is no longer valid in this microscopic world, and the AB effect now plays an essential role in understanding the performance of ultra-microscopic devices. It was recently reported[38)] that metal carbon nanotubes can be changed to semiconductors due to the AB effect, because a phase factor is added to the wavefunction, thus changing even the band structures.

As these examples show, the AB effect is invading the more macroscopic and more practical world, although the AB effect has not yet been confirmed in an exact sense, except for the electron beam experiments.

Applications of the AB effect in electromagnetic-field observation. The AB effect principle has been used to observe microscopic distributions of electromagnetic fields by detecting the phase of the transmitted electron beam. More specifically, the thickness distribution of a specimen uniform in material can be observed as the thickness contours in the interference micrograph obtained through an electron holography process[39)] because the phase of an electron wave is shifted by the inner potential of the specimen when the wave passes through it.

Relative phase shifts can be detected from the conventional interference pattern with a $2\pi/4$ precision, but the precision increases up to $2\pi/100$ by using a phase-amplification technique peculiar to holography. In

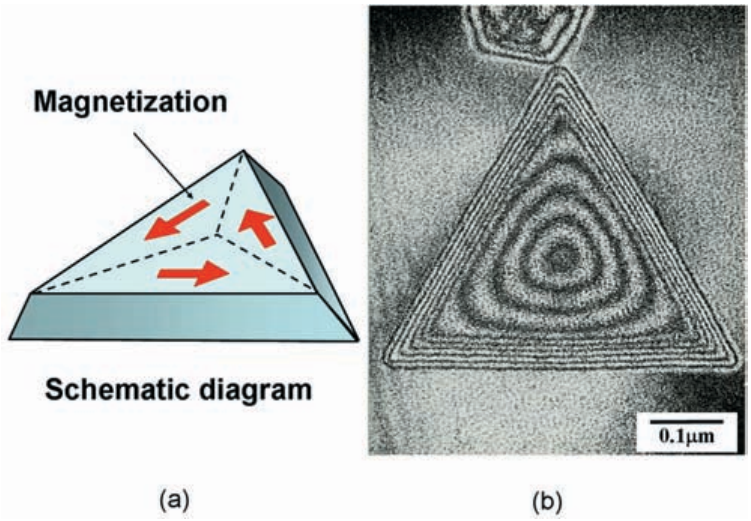

Fig. 3. Cobalt fine particle. (a) Schematic diagram. (b) Interference micrograph.

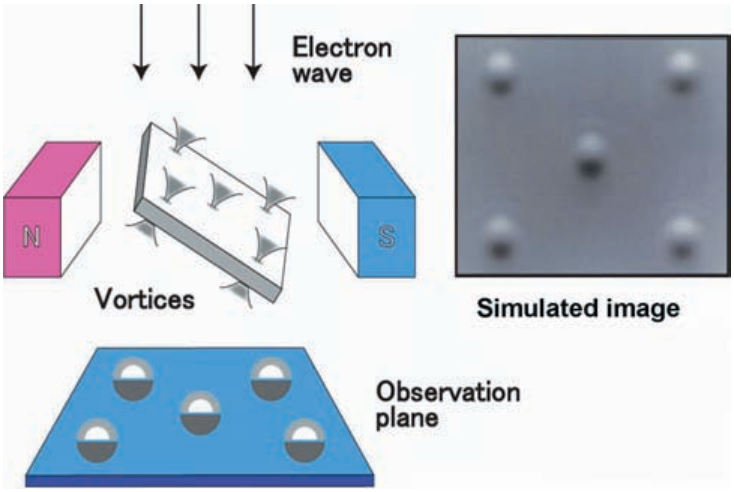

Fig. 4. Principle behind vortex observation.

fact, this technique has helped detect thickness changes due to monatomic steps[40] and carbon nanotubes.[41]

(A) Magnetic lines of force. In the case of pure magnetic fields, the phase shift is produced by vector potentials. When the phase distribution is displayed as a contour map, the micrograph can be interpreted in the following straightforward way.[16]

1. Contour fringes in the interference micrograph indicate magnetic lines of force, since no relative phase shift is produced between the two beams passing through two points along a magnetic line.

2. Contour fringes show magnetic flux in units of h/e, since the relative phase shift between two beams enclosing a magnetic flux of h/e is 2π.

An example observation of magnetic lines of force inside a ferromagnetic fine particle is shown in Fig. 3. Only the triangular outline of this particle can be observed by electron microscopy. In its interference micrograph, two kinds of contour fringes appear: narrow fringes parallel to the edges indicate the thickness contours in 200 Å units, and circular fringes in the inner region indicate in-plane magnetic lines of force in $h/(2e)$

flux units since the micrograph is amplified two times and the specimen thickness is uniform there.

(B) Vortices in superconductors. Interference microscopy is not the only technique that can be used to visualize the phase distribution. For example, some kind of a phase object can be observed in an out-of-focus image because the phase change is transformed into an intensity change when the image is defocused. A quantized vortex in a superconductor, which acts as a pure weak phase object to an illuminating electron beam, has actually been visualized as a spot in a defocused image, or a Lorentz micrograph.[22)]

The experimental arrangement for observing vortices in a superconducting thin film is shown in Fig. 4. When a magnetic field is applied to the tilted film, vortices are produced. Electrons passing through the film are phase-shifted by the magnetic fluxes of the vortices due to the AB effect. The vortices can be observed by simply defocusing the electron microscopic image. That is, when the intensity of the electrons is observed in an out-of-focus plane, a vortex appears as a pair of bright and dark contrast features (Fig. 4).

Therefore, we can observe the dynamics of vortices in real time by applying Lorentz microscopy, such as the behaviors of vortices at pinning centers and surface steps under various conditions of sample temperatures and applied magnetic fields. In fact, vortices move in interesting ways as if they were living organisms.

An interesting example[42)] is shown in Fig. 5, where two kinds of vortex images appear in a single field of view. They are vortices and antivortices produced in a niobium thin film when the 100 G magnetic field applied to the film is suddenly reversed and its magnitude increases. The original vortices are leaving the film, but cannot instantly do so since they are pinned down by defects, while the oppositely oriented vortices begin to penetrate the film from its edges. Where two streams of vortices and antivortices collide head-on, the vortex-antivortex pairs of the heads of the two streams annihilate each other. The direct observation of the pair annihilation can simulate that of particles and antiparticles.

Artificial pinning centers can be produced by a focused ion beam. When they form regular lattices, the macroscopic measurement indicates that the critical current has peaks at specific values of the magnetic field. We microscopically investigated this matching effect by directly observing vortex behavior.[43)]

A regular array of "red" artificial defects was produced in a niobium thin film, and the vortex configuration was investigated by Lorentz microscopy under specific magnetic fields.

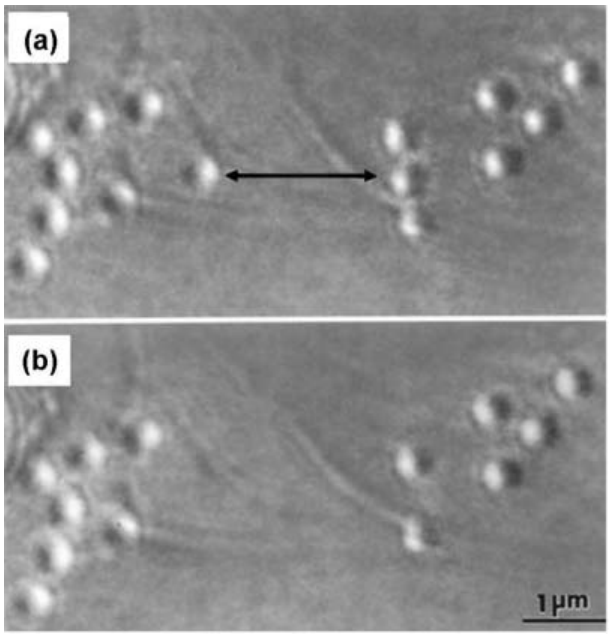

Fig. 5. Annihilation of vortices and antivortices in a thin film of niobium. (a) Before annihilation. (b) After annihilation.

Some of the micrographs are shown in Fig. 6, where pink dots indicate the locations of defects, and the larger blue spots vortex images. The vortices form regular and rigid lattices under the matching magnetic field ($H = H_1$), four times the matching field ($H = 4H_1$), and even 1/4th the matching field ($H = 1/4H_1$).

The reason the critical current has peaks at these specific fields is now evident; even if a vortex is depinned from one pinning site, it cannot find a stable "vacant site" to move to because the vortices form regular and rigid lattices. As a result, stronger forces are needed to move them, thus producing the matching effect of the critical current.

(C) Pinning of vortices by columnar defects. High-T_c superconductors have been expected to be practically used, but the critical current is, in general, very low because both the high temperature operation and the layered structure of the materials enable the vortices to easily move. To directly observe the unconventional behavior of vortices in high-T_c superconductors, we developed a 1-MV field-emission electron microscope[29)] (Fig. 7). The 1-MV electrons are needed to observe the vortices because the electrons can penetrate a film thicker than the magnetic radius (penetration depth) of vortices in high-T_c superconductors. With

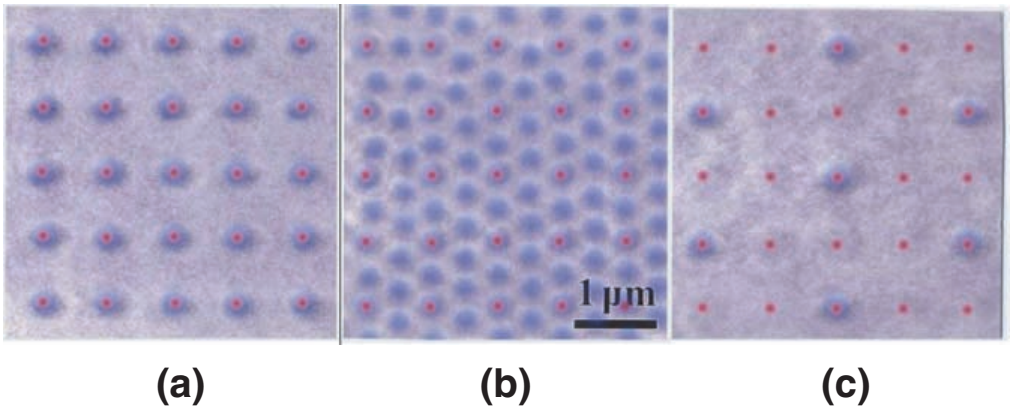

Fig. 6. Lorentz micrographs of vortices. (a) $H = H_1$. (b) $H = 4H_1$ (H_1: matching magnetic field). (c) $H = 1/4H_1$.

Fig. 7. 1-MV field-emission transmission electron microscope.

this microscope, we first observed the internal behavior of vortices inside high-T_c Bi-2212 thin films.[23)]

The columnar defects, which are produced by the irradiation of high-energy heavy ions and are considered optimal pinning traps for vortices in layered structure materials, are produced in Bi-2212 films in a tilted direction (see the electron micrograph shown in Fig. 8(a)). The tilted columns can be seen as tiny lines. When these images are defocused, they are blurred and, eventually, completely disappear by spreading out. However, when they are defocused even further, vortex images appear, since they are produced by the phase contrast. The resultant Lorentz micrograph of vortices is shown in Fig. 8(b). Some vortices are trapped at columnar defects and others are untrapped. The elongated images indicated by the arrows in the micrograph are produced only at the locations of the columnar defects and correspond to vortices trapped along the tilted columns.

We also confirmed this in the simulation. The images of the untrapped vortex lines perpendicular to the film plane are circular spots having bright and dark regions. Vortex images located at the positions of the columnar defects are elongated spots with lower contrasts, since these vortex lines are trapped at columnar defects tilted 70°.

The circular images are produced in regions without defects in Fig. 8(b), and therefore, correspond to vortices perpendicularly penetrating into the film. An example of these vortices in a wider field of view is shown in Fig. 9. Red vortex-images correspond to the vortices trapped by the columnar defects. When a driving force is applied, the difference in their pinning forces becomes evident. Untrapped vortices soon begin to move, but trapped vortices do not. This has enabled us to use these different vortex images to investigate whether vortices are trapped or not under various conditions,[23)] even when they are moving.

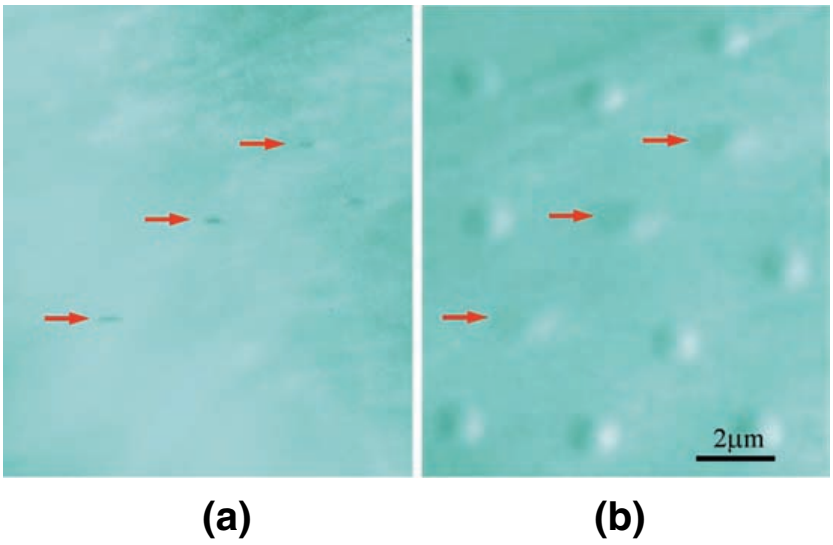

Fig. 8. Comparison of columnar-defect images and vortex images in Bi-2212 thin film. (a) Electron micrograph. (b) Lorentz micrograph.

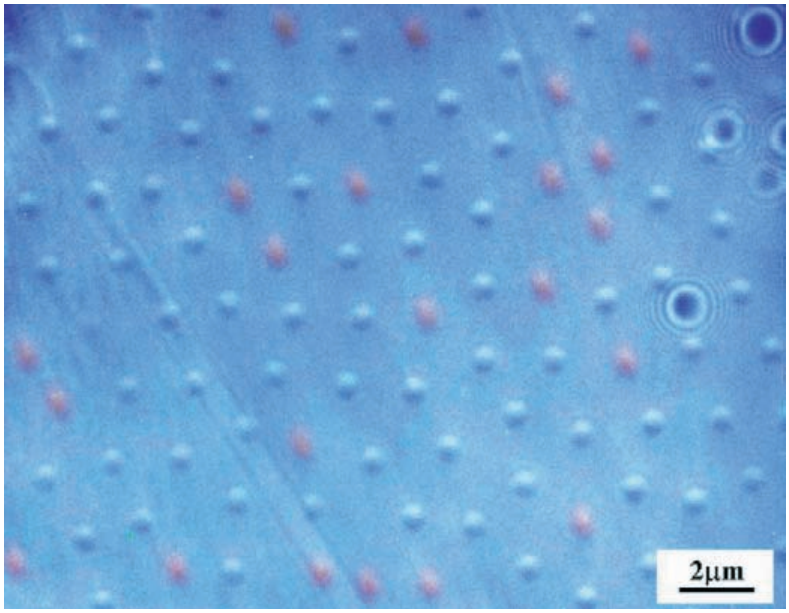

Fig. 9 Lorentz micrograph of vortices in high-T_c Bi-2212 superconducting thin film with tilted columnar defects. The red vortex-images correspond to vortices trapped at the defects.

(D) Unusual arrangements of vortices in high-T_c superconductors. Vortices usually form a closely packed triangular lattice. This is the case even for anisotropic high-T_c superconductors, as long as the magnetic field is directed along the anisotropy c-axis.

When the magnetic field is strongly tilted away from the c-axis, however, Bitter images show that the vortices no longer form a triangular lattice. Instead, in the case of $YBaCu_3O_{7.8}$ (YBCO), they form arrays of linear chains along the direction of the tilting field and alternating

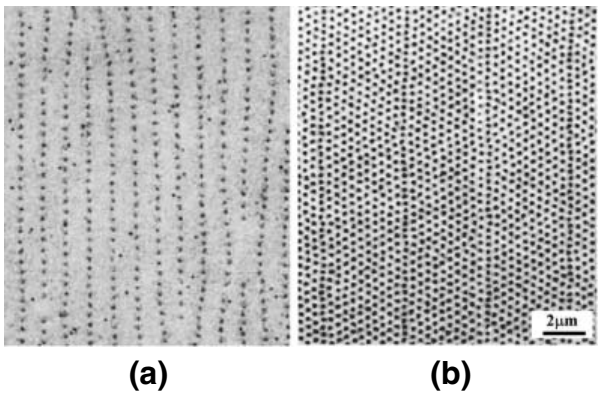

Fig. 10. Bitter patterns of vortices at tilted magnetic fields. (a) YBCO. (b) Bi-2212.

domains of chains and triangular lattices for Bi-2212[44),45)] (Fig. 10). While the chain state in YBCO was explained by the tilting of the vortex lines within the framework of the anisotropic London theory,[46)] the chain-lattice state in Bi-2212 has long been an object of discussion. For example, it has been attributed to two sets of vortex lines with different orientations,[47)] one set forming chains and the other forming triangular lattices.

Koshelev[48)] proposed an interesting model for the chain-lattice state; elliptical Josephson vortices penetrate between the layer planes in Bi-2212 and vortices that perpendicularly intersect the Josephson vortices form chains with the rest of the vortices forming triangular lattices. However, no direct evidence for such mechanism was experimentally given because of the lack of methods for observing the arrangements of vortex lines *inside* superconductors. In addition, this model used to be thought to be difficult to accept, since no interaction takes place between the two perpendicular magnetic fields. However, Koshelev considered the second-order approximation and determined an energy reduction in this vortex arrangement. As a result of the interaction between the two kinds of vortices, a vertical vortex line winds a little bit in the opposite directions above and below the crossing Josephson vortex, since the circulating supercurrent around the Josephson vortex exerts Lorentz forces onto the vertical vortex line.

Lorentz microscopy with our 1-MV electron microscope has been used for determining whether or not vortex lines in the chain states inside high-T_c superconductors are tilted or not. For YBCO, we found that vortices tilted together in the direction the applied magnetic field tilted.[28)] This conclusion is evident from the obtained Lorentz micrographs in Fig. 11, in which the vortex images become more elongated and together form linear chains as the tilting angle of the magnetic field increases. When the tilt angle becomes larger than 75°, the vortex images begin to elongate and, at the same time, form arrays of linear chains. This implies that vortices in YBCO are produced by some attractive force between the tilted vortex lines to form chains.

For our Bi-2212, Lorentz microscopy observation under various defocusing conditions showed that neither chain- nor lattice-vortices tilted, but both stood perpendicular to the layer plane,[45)] as shown in Fig. 12(a). If vortex lines are strongly tilted at an angle comparable to that of the applied magnetic field, the vortex images should be elongated as shown in the inset of Fig. 12(a).

Our finding that both chain- and lattice-vortices stand straight and do not tilt is clear evidence of the Koshelev mechanism. Although the clearest evidence for this model would of course be if the Josephson vortices were directly observed along the chain vortices. However, the magnetic field of a Josephson vortex widely extends between the layers and, therefore, makes it difficult to detect with our method. In fact, we could not directly observe Josephson vortices, but we found evidence for their existence: we observed vertical vortices penetrating into the sample always along some straight lines. These straight lines must be determined by the Josephson vortices.

An example of this is shown in Fig. 13. When we apply an in-plane magnetic field, no vortex images can be seen in the Lorentz micrograph [Fig. 13(a)]. However, when a perpendicular magnetic field B_p is additionally applied and slowly increased, images of vertical vortices began to appear in this field of view. They do not appear in the triangular-lattice form but only along straight lines, indicated by white lines in Fig. 13(b), which are considered to be determined by Josephson vortices. Since vortices are always located along straight lines, even at large intervals between the lines, we can find no other reason for the production of chain vortices than the assumption that vertical vortices crossing Josephson vortices form chains as illustrated in Fig. 12(b). Above B_p = 1 G, vertical vortices also appear between the chain vortices, as shown in Fig. 13(c).

We also found that only the images of chain vortices in Bi-2212 begin to disappear at temperatures much lower than the critical temperature T_c.[27)] An example is shown in Fig. 14. The chain of vortices in this case began to disappear at 50 K, *i.e.*, well below T_c (83 K). This does not mean that the vortices themselves disappear for the

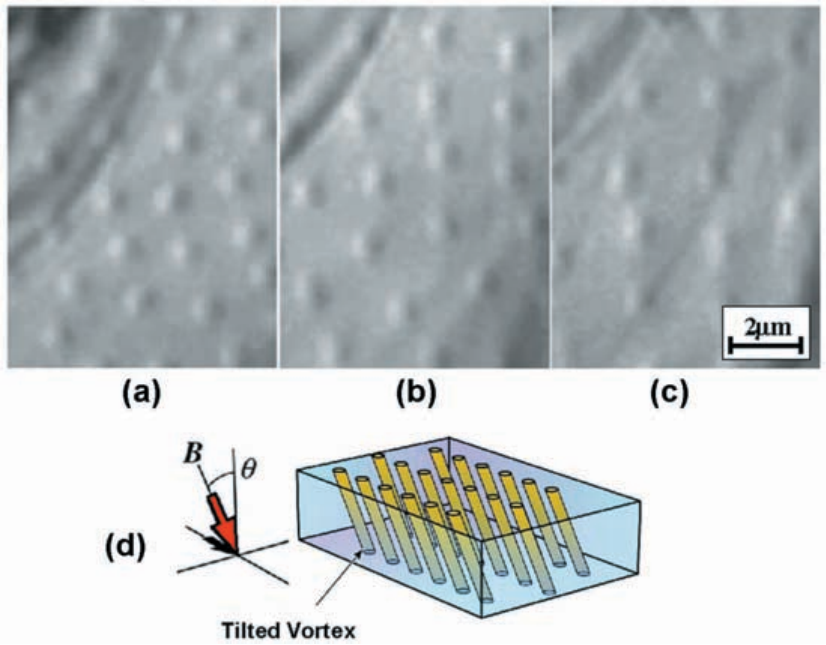

Fig. 11. Lorentz micrographs of vortices in YBCO film sample at tilted magnetic fields (T = 30 K; B_p = 3 G). (a) $\theta = 75^\circ$. (b) $\theta = 82^\circ$. (c) $\theta = 83^\circ$. (d) Schematic of tilted vortex lines. When the tilt angle becomes larger than 75°, the vortex images begin to elongate and, at the same time, to form arrays of linear chains. This implies that chain vortices in YBCO are produced by some attractive force between tilted vortex lines.

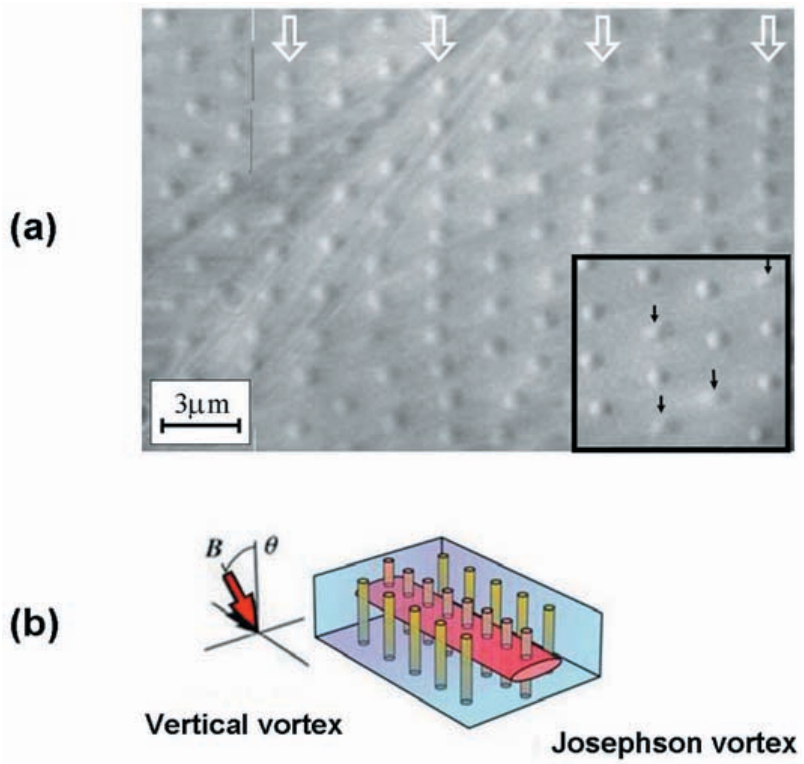

Fig. 12. Chain-lattice state of vortices at tilted magnetic field in Bi-2212. (a) Lorentz micrograph (T = 50 K and B = 50 G). (b) Schematic. The chains are indicated by white arrows in (a). If vortex lines are tilted at an angle comparable to the tilt angle of the magnetic field, *i.e.*, 85°, the vortex images must be elongated and weak in contrast under this defocusing condition. Since the images of chain vortices, as well as those of lattices vortices, are not elongated but circular, all the vortex lines are not tilted, but perpendicular to the layer plane. If tilted, the vortex line images become elongated as shown in the inset in (a).

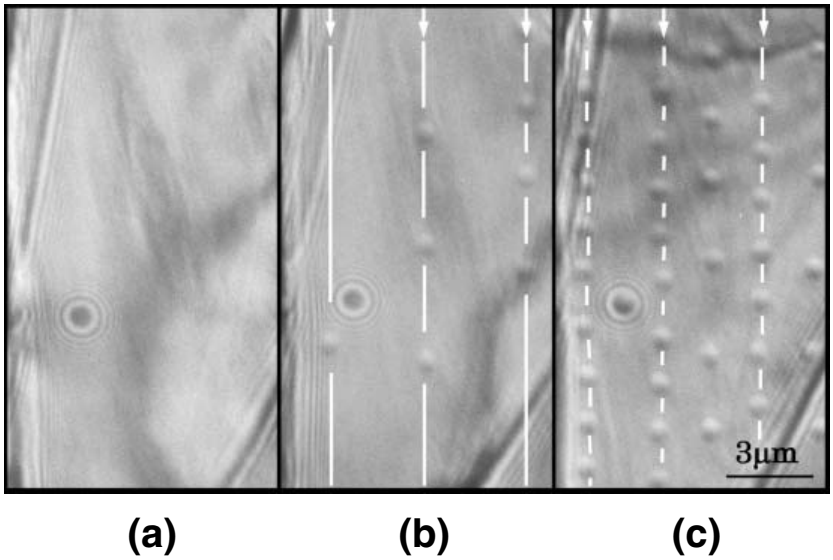

Fig. 13. Series of Lorentz micrographs of vortices in Bi-2212 film sample when magnetic field B_p perpendicular to layer plane begins to be applied and increases at fixed in-plane magnetic field of 50 G at T = 50 K. (a) B_p = 0 G. (b) B_p = 0.2 G. (c) B_p = 1 G.

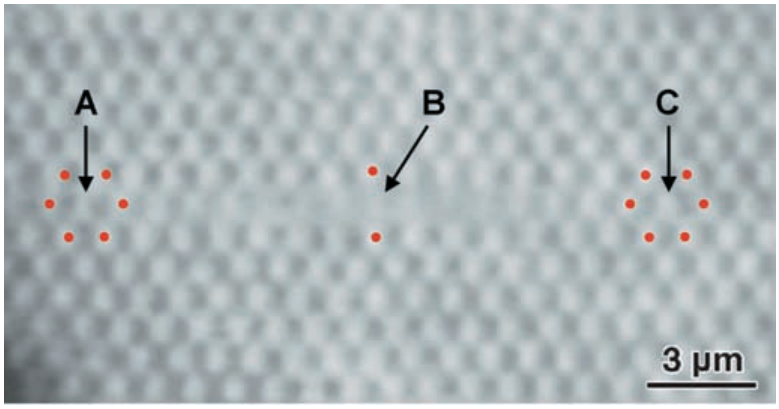

Fig. 14. Lorentz micrograph of disappearing chain vortices in Bi-2212 (T = 57 K, B_p = 8 G, θ = 80°). We attribute the disappearance of the vortex images to the synchronous oscillation of vortices between node vortices A and C along the chain direction, just like a coupled oscillation.

following two reasons. One is that vortex images gradually fade away with rising temperatures. The other is that the vortex images, even along a single chain, partially disappear depending on the relative positions with the surrounding lattice vortices. That is, in Fig. 14, vortices A and C can be clearly seen in the chain, but vortices that are far from it begin to disappear. Vortices A and C are located "stably" in the midst of the six surrounding vortices indicated by the red points in the figure, while vortex B is sandwiched "unstably" between the two vortices above and below.

This vortex arrangement may be stable at low temperatures, but at high temperatures where vortices vibrate thermally, vortex B begins to oscillate back and forth, like pinballs connected by springs on incommensurate periodic potentials, as in the Frenkel-Kontorova

model. We attributed the disappearance of chain vortices possibility to such longitudinal oscillations of vortices along chains.

Conclusion. Thanks to recent developments in advanced technologies such as coherent electron beams, highly sensitive electron detectors, and photolithography, some of the experiments that were once regarded as "Gedanken" experiments can now be carried out. In addition, the wave nature of electrons is utilized to observe microscopic objects previously unobservable. Some examples are the quantitative observation of both the microscopic distribution of magnetic lines of force in *h/e* units by interference microscopy and the dynamics of quantized vortices in superconductors by Lorentz microscopy. This measurement and observation technique is expected to play a more important role in future research and development in nano-science and technology.

References

1) Aharonov, Y., and Bohm, D. (1959) Phys. Rev. **115**, 485-491.
2) Ehrenberg, W., and Siday, R. W. (1949) Proc. Phys. Soc. London B **62**, 8-21.
3) Wu, T. T., and Yang, C. N. (1975) Phys. Rev. D **12**, 3845-3857.
4) Bocchieri, P., and Loinger, A. (1978) Nuovo Cimento **47A**, 475-482.
5) Peshkin, M., and Tonomura, A. (1989) Lecture Notes in Physics, vol. 340, Springer, Heidelberg.
6) Chambers, R. G. (1960) Phys. Rev. Lett. **5**, 3-5.
7) Fowler, H. A., Marton, L., Simpson, J. A., and Suddeth, J. A. (1961) J. Appl. Phys. **32**, 1153-1155.
8) Möllenstedt, G., and Bayh, W. (1962) Phys. Bl. **18**, 299-305.
9) Boersch, H., Hamisch, H., and Grohmann, K. (1962) Z. Phys. **169**, 263-272.
10) Roy, S. M. (1980) Phys. Rev. Lett. **44**, 111-114.
11) Bocchieri, P., and Loinger, A. (1981) Lett. Nuovo Cimento **30**, 449-450.
12) Tonomura, A., Matsuda, T., Suzuki, R., Fukuhara, A., Osakabe, N., Umezaki, H., Endo, J., Shinagawa, K., Sugita, Y., and Fujiwara, H. (1982) Phys. Rev. Lett. **48**, 1443-1446.
13) Tonomura, A., Umezaki, H., Matsuda, T., Osakabe, N., Endo, J., and Sugita, Y. (1983) Phys. Rev. Lett. **51**, 331-334.
14) Tonomura, A., Osakabe, N., Matsuda, T., Kawasaki, T., Endo, J., Yano, S., and Yamada, H. (1986) Phys. Rev. Lett. **56**, 792-795.
15) Osakabe, N., Matsuda, T., Kawasaki, T., Endo, J., Tonomura, A., Yano, S., and Yamada, H. (1986) Phys. Rev. A **34**, 815-822.
16) Tonomura, A., Matsuda, T., Endo, J., Arii, T., and Mihama, K. (1980) Phys. Rev. Lett. **44**, 1430-1433.
17) Tonomura, A. (1999) Electron Holography. 2nd ed., Springer, Heidelberg.
18) Kuper, C. G. (1980) Phys. Lett. **794**, 413-416.
19) Yang, C. N. (1984) *In* Proc. Int. Symp. on Foundations of Quantum Mechanics, Tokyo, 1983 (eds. Kamefuchi, S., Ezawa, H., Murayama, Y., Nomura, S., Ohnuki, Y., and Yajima, T.). Phys. Society of Japan, Tokyo, p. 27.
20) Tonomura, A., Matsuda, T., Endo, J., Arii, T., and Mihama, K. (1986) Phys. Rev. B **34**, 3397-3402.
21) Bonevich, J. E., Harada, K., Matsuda, T., Kasai, H., Yoshida, T., Pozzi, G., and Tonomura, A. (1993) Phys. Rev. Lett. **70**, 2952-2955.
22) Harada, K., Matsuda, T., Bonevich, J., Igarashi, M., Kondo, S., Pozzi, G., Kawabe, U., and Tonomura, A. (1992) Nature **360**, 51-53 (5 November).
23) Tonomura, A., Kasai, H., Kamimura, O., Matsuda, T., Harada, K., Nakayama, Y., Shimoyama, J., Kishio, K., Hanaguri, T., Kitazawa, K. *et al.* (2001) Nature **412**, 620-622 (9 August).
24) Tonomura, A., Fukuhara, A., Watanabe, H., and Komoda, T. (1968) Jpn. J. Appl. Phys. **7**, 295.
25) Tonomura, A., Matsuda, T., Endo, J., Todokoro, H., and Komoda, T. (1979) J. Electron Microsc. **28**, 1-11.
26) Kawasaki, T., Matsuda, T., Endo, J., and Tonomura, A. (1990) Jpn. J. Appl. Phys. **29**, L508- L510.
27) Matsuda, T., Kamimura, O., Kasai, H., Harada, K., Yoshida, T., Akashi, T., Tonomura, A., Nakayama, Y., Shimoyama, J., Kishio, K. *et al.* (2001) Science **294**, 2136-2138 (7 December).
28) Tonomura, A., Kasai, K., Kamimura, O., Matsuda, T., Harada, K., Yoshida, T., Akashi, T., Shimoyama, J., Kishio, K., Hanaguri, T. *et al.* (2002) Phys. Rev. Lett. **88**, 237001-237005.
29) Kawasaki, T., Yoshida, T., Matsuda, T., Osakabe, N., Tonomura, A., Matsui, I., and Kitazawa, K. (2000) Appl. Phys. Lett. **76**, 1342-1344.
30) Konopinski, K. J. (1978) Am. J. Phys. **46**, 499-502.
31) Yang, C. N. (1996) *In* Quantum Coherence and Decoherence (eds. Fujikawa, K., and Ono, Y. A.). North-Holland Delta Series, Elsevier, Amsterdam, pp. 307-314.
32) Maxwell, J. C. (1856) Trans. Camb. Phil. Soc. **10**, 27-83.
33) For example, see: Heaviside, O. (1893-1912) Electromagnetic Theory. 3 vols. London: Electrician Co. Repr., New York: Chelsea, 1971.
34) Hertz, H. R. (1884) Wiedemann's Annalen **23**, 84-103.
35) Weyl, H. (1919) Ann. der Physik **59**, 101-133.
36) Webb, R. A., Washburn, S., Umbach, C. P., and Laibowitz, R. B. (1985) Phys. Rev. Lett. **54**, 2696-2699.
37) Bachtold, A., Strunk, C., Salvetat, J. P., Bonard, J. M., Forro, L., Nussbaumer, T., and Schönenberger, C. (1999) Nature **397**, 673-675.
38) Minot, E. D., Yalsh, Y., Sazonova, V., and McEuen, P. L. (2004) Nature **428**, 536-539.
39) Tonomura, A., Endo, J., and Matsuda, T. (1979) Optik **53**, 143-146.
40) Tonomura, A., Matsuda, T., Kawasaki, T., Endo, J., and Osakabe, N. (1985) Phys. Rev. Lett. **54**, 60-62.
41) Ru, Q., Endo, J., Tanji, T., and Tonomura, A. (1991) Appl. Phys. Lett. **59**, 2372-2374.

42) Harada, K., Kasai, H., Matsuda, T., Yamasaki, M., and Tonomura, A. (1997) J. Electron Microsc. **46**, 3227-3232.
43) Harada, K., Kamimura, O., Kasai, H., Mastuda, T., and Tonomura, A. (1996) Science **274**, 1167-1169.
44) Bolle, C. A., Gammel, P. L., Grier, D. G., Murray, C. A., Bishop, D. J., Mitzi, D. B., and Kapitulnik, A. (1991) Phys. Rev. Lett. **66**, 112-115.
45) Gammel, P. L., Bishop, D. J., Rice, J. P., and Ginsberg, D. M. (1992) Phys. Rev. Lett. **68**, 3343-3346.
46) Buzdin, A. I., and Simonov, A. Y. (1990) JETP Lett. **51** 191-195.
47) Grigorieva, I. V., and Steeds, J. W. (1995) Phys. Rev. **B51**, 3765-3771.
48) Koshelev, A. E. (1999) Phys. Rev. Lett. **83**, 187-190.

(Received Dec. 8, 2005; accepted Feb. 13, 2006)

Profile

Akira Tonomura was born in 1942. After he graduated from the University of Tokyo, Department of Physics, in 1965, he joined Hitachi, Ltd. He has been engaged in experimental researches on electron physics using electron microscopes. From 1973 he stayed for one year at Tübingen University to research on electron interferometry. He is now a fellow of Hitachi, Ltd., and concurrently a group director of Riken, and also principal investigator of OIST. He received his Doctor of Engineering from Nagoya University in 1975 and Ph. D from Gakushuin University in 1993. He was awarded the Nishina Memorial Prize in 1982, the Asahi Prize in 1987, the Japan Academy Prize and Imperial Prize in 1991, and the Benjamin Franklin Medal in Physics from the Franklin Institute in 1999. He was elected as a foreign associate of the National Academy of Sciences in the United States in 2001 and a member of Science Council of Japan in 2005. He is recognized for his pioneering work in the new fields of electron holography which was made possible by the development of a "coherent" field-emission electron beam. This method is used for the direct observation of both microscopic electromagnetic fields and magnetic vortices in superconductors, and the verification of fundamental phenomena in quantum mechanics such as Aharonov-Bohm effect and single-electron build-up of an interference pattern.